(65) ANALYSIS OF FACTORS REGULATING ALGAL BLOOM IN MIKAWA BAY USING EUTROPHICATION MODEL

富栄養化モデルを用いた三河湾の藻類増殖要因に関する解析

G.A. ANGGARA KASIH* and Toshihiro KITADA**
アンガラカシ*、北田敏廣**

Abstract; On many marine systems, nutrient has been identified as the pollutant of concern, and is believed to stimulate the excessive alga growth. In this study, eutrophication model was used to clarify the factors regulating the chlorophyll-a production in Mikawa Bay. We have examined the temporal variations of total nitrogen (TN), chlorophyll-a, and bay water temperature as well as those of input river flow rate and tidal height for two months from May to early July in 1998, during which algal bloom events occurred. The obtained results are as follows: (1) near at the bottom in the inner bay, TN concentration started to increase after 1 May due to enhanced TN release from the sediment, which followed by chlorophyll-a, (2) TN and chlorophyll-a near the surface layer were strongly affected by river flow rate; the TN concentration showed its sharp increase when the river flow increased, and in contrast the chlorophyll-a was decreased; they were because of high TN and low chlorophyll-a concentrations in the river water, (3) the high chlorophyll-a concentration at the event was caused by combination of the high TN input through increased river flow rate before the event and the subsequent weak ventilation of the inner bay water under the neap tide condition, and (4) the weak ventilation was further enhanced by strong stable stratification in the inner bay.

Key words; coastal eutrophication, nutrient, chlorophyll-a, ecological model, Mikawa Bay

1. INTRODUCTION

Mikawa Bay is a semi enclosed bay located in the middle of Japan and approximately 700.000 people live near the watershed. The watershed area has been used intensively for agricultural and livestock production, from which watershed nutrient has been loaded into Atsumi Bay (the eastern half of Mikawa Bay) through two major rivers of Toyokawa and Umedagawa, and the plants of municipal waste water treatment at Noda and Nakashima.

In the last four decades, increased human activities in the watershed and the bay area have resulted in damaged the ecosystem of Mikawa Bay; they caused poor water quality and losses of the aquatic habitat in the bay. On many marine systems, nutrient has been identified as the pollutant of concern, and is believed to stimulate the excessive alga growth.

Modeling study to look at the mechanism of eutrophication and formation of oxygen depleted water mass in Ise and Mikawa Bay has been reported by many researchers such as Suzuki and Terasawa (1997)[1], Sohma et al. (2001)[2], etc. In particular, Suzuki and Terasawa[1] performed 3 dimensional fluid dynamic calculation combined with a marine ecological model for Ise and Mikawa Bay; they predicted typical flow patterns in the area in summer season, and showed low ventilation of sea water in both bays. They further tried to investigate effects of the two parameters of both prevailing wind and river flow rate on the ventilation rate. In their study, they chose rather averaged values for the forcing parameters such as constant wind and constant river flow rate, though it is expected that, in reality, the wind shows quite clear diurnal variation in its direction and speed under summertime-typical high pressure system, and river flow rate can vary day-by-day depending on precipitation history.

In this study, we tried to clarify relation between algal bloom and factors such as river flow rate, temperature, and tide by looking at month long simulation results performed with use of time-varying forcing parameters of meteorology, river flow rate, and tide. For this purpose, we applied a model of CE-Qual-W2 [3] for four month long simulation starting from April in1998 for Atsumi Bay, which is the eastern half of Mikawa Bay; and a part of the results, i.e. those for June and early July, was used for the analysis. As will be briefly described later in 2.1, CE-Qual-W2 laterally integrates three-dimensional partial differential equations for both

* 豊橋技術科学大学大学院工学研究科博士課程 (Doctor Course Student, Toyohashi University of Technology)
**豊橋技術科学大学エコロジー工学系 教授 (Prof., Dept of Ecological Engineering, Toyohashi University of Technology)

fluid dynamics and transport/chemistry of water quality-related state variables, thus leading them to their two-dimensional forms.

The two-dimensional, but with-detailed-chemistry, model allowed longer term simulation to fully see the effects of past memory of the forcing parameters on the water quality. In the simulation we assumed the calculation domain of Atsumi Bay can be modeled as two-dimensional space.

In our previous study[4, 5], we used CE-Qual-W2 for three year simulation (from April, 1998 to March, 2001) to see statistical correlation between chlorophyll-a and total nitrogen (TN), total phosphorus (TP) etc., and quantitatively discussed that to reduce chlorophyll-a concentration in the bay, sediment control such as suppression of TN release from the sediment is more effective than the reduction of TN loading from land area.

2. METHOD

2.1 Model equations

Both hydrodynamic and water quality variables in the bay were simulated using CE-Qual-W2 model[3]. Governing equations in the model are laterally integrated; thus the calculation is performed in two-dimensional space with longitudinal and vertical axes. The hydrodynamic model includes turbulence model to describe vertical eddy viscosity/diffusivity, which are calculated using Prandtl's mixing length concept. Eddy viscosity varies both in time and space according to the mixing energy available from shear of wind and shear of flow velocity in the water; the effect of vertical density stratification on production/destruction of turbulent kinetic energy is also considered. Eddy diffusivities are evaluated by multiplying the eddy viscosity by some constants.

In addition to the hydrodynamic aspects, thirteen state variables are considered in water quality algorithm: chlorophyll-a, ammonium (NH_4^+), nitrate (NO_3^-), orthophosphate (PO_4^{3-}), dissolved silica, particulate silica, labile dissolved organic matter (LDOM), labile particulate organic matter (LPOM), refractory dissolved organic matter (RDOM), refractory particulate organic matter (RPOM), chemical oxygen demand (COD), sediment and salinity. The relationships among these state variables are schematically illustrated in Fig. 2. Symbols used in the following equations are listed in Table 1. The following equations of (1), (5), (6), and (7) show bio-geo-chemical kinetics for selected state variables. In the simulation by CE-Qual-W2, the terms on the right hand side of these equations are incorporated as chemical kinetic part into unsteady two-dimensional partial differential equations of transport/chemistry for state variables.

The growth rate of phytoplankton is given by:

$$\frac{\partial \Phi_a}{\partial t} = (K_{ag} - K_{ar} - K_{ae} - K_{am} - \frac{\omega_a}{\Delta_z})\Phi_a \qquad (1)$$

where the coefficient of alga growth rate (K_{ag}) is computed with a maximum growth rate (K_{agmax}) modified by temperature, light, and nutrient availability as Eq. 2:

$$K_{ag} = \gamma_{ar}\gamma_{af}\lambda_{min}K_{agmax} \qquad (2)$$

where λ_{min} stands for limiting growth factor which is determined as the minimum value between factors related to nutrient concentrations λ_i in Eq. 4 and available sunlight intensity λ_I in Eq. 3. The Steele function[3] is used to calculate the light limitation of alga growth, and is given as follows:

$$\lambda_I = \frac{I}{I_s}\exp(-\frac{I}{I_s}+1) \qquad (3)$$

where the saturating light intensity (Is) is assumed to be 45% of the available photosynthetically active radiation. Rate multipliers limiting alga growth due to concentrations of phosphorus and nitrogen are computed using the Monod relationship:

$$\lambda_i = \frac{\Phi_i}{P_i + \Phi_i} \qquad (4)$$

where the subscript "i" represents either phosphorus or nitrogen. The mass of alga was estimated from chlorophyll-a by assuming that alga biomass can be obtained by multiplying the chlorophyll-a concentration by a factor of 67 as recommended by the Ce-Qual-W2 user manual[3].

Two mineral nitrogen forms are considered in the model: ammonium and nitrate. External load provides the ultimate source of nitrogen to the system. Inorganic nitrogen is incorporated into alga during their growth and is released as ammonium and nitrate through respiration.

The rate equation for nitrate (Φ_{NO3}) is expressed as follows:

$$\frac{\partial \Phi_{NO3}}{\partial t} = K_{NH4}\gamma_{NH4}\Phi_{NH4} - K_{NO3}\gamma_{NO3}\Phi_{NO3} - K_{ag}\delta_N\Phi_a\left(1 - \frac{\Phi_{NH4}}{\Phi_{NH4} + \Phi_{NO3}}\right) \quad (5)$$

In anoxic water, nitrate is lost to nitrogen gas through denitrification. Particulate nitrogen that settles to the sediment is mineralized and recycled to the water column primarily as ammonium.

The rate equation for ammonium (Φ_{NH4}) is as follows:

$$\frac{\partial \Phi_{NH4}}{\partial t} = K_{ar}\delta_N\Phi_a - K_{ag}\delta_N\Phi_a\frac{\Phi_{NH4}}{\Phi_{NH4} + \Phi_{NO3}} + K_{LDOM}\delta_N\gamma_{om}\Phi_{LDOM} + K_{LPOM}\delta_N\gamma_{om}\Phi_{LPOM}$$
$$+ K_{RPOM}\delta_N\gamma_{om}\Phi_{RPOM} + K_{RDOM}\delta_N\gamma_{om}\Phi_{RDOM} + K_s\delta_N\gamma_{om}\Phi_s + Sed_{NH4}\gamma_{om}A_s + K_{NO3}\gamma_{NO3}\Phi_{NO3} \quad (6)$$
$$- K_{NH4}\gamma_{NH4}\Phi_{NH4}$$

Phosphorus is assumed to be available completely as orthophosphate for uptake by phytoplankton and released through respiration. A portion of the phosphorus PO_4^{3-} settles to the sediment. In the sediment, phosphorus is mineralized and recycled to the water column.

The rate equation for phosphorus (Φ_p) is given as follows:

$$\frac{\partial \Phi_p}{\partial t} = (K_{ar} - K_{ag})\delta_p\Phi_a - K_{LDOM}\delta_p\gamma_{om}\Phi_{LDOM} + K_{LPOM}\delta_p\gamma_{om}\Phi_{LPOM} +$$
$$K_{RPOM}\delta_p\gamma_{om}\Phi_{RPOM} + K_{RDOM}\delta_p\gamma_{om}\Phi_{RDOM} + K_s\delta_p\gamma_{om}\Phi_s + S_{od}\gamma_{om}A_s - \frac{P_p}{\Delta z}\Phi_p \quad (7)$$

Detailed description of the equations for other state variables used in the model can be found in Cole and Wells (2000) [3].

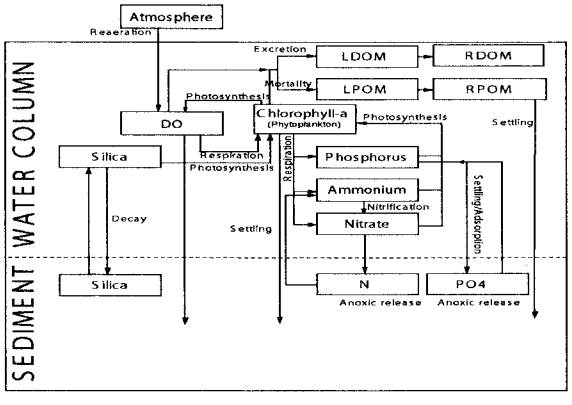

Fig. 2. Block diagram showing relationships among state variables. "Phosphorus" represents "Total Phosphorus (TP)" used in the text; "TP" includes PO_4. The "Total Nitrogen (TN)" in the text represents ammonium, nitrate, and others.

Table 1: List of symbols and description for water quality calculation

A_s	The sediment area, m^2
I	Available light, Wm^{-2}
I_s	Saturating light intensity at max photosynthetic rate, Wm^{-2}
K_{ae}	The alga excretion rate, s^{-1}
K_{ag}	The alga growth rate, s^{-1}
K_{agmax}	The maximum alga growth rate, s^{-1}

K_{am}	The alga mortality rate, s^{-1}
K_{ar}	The alga respiration rate, s^{-1}
K_{LDOM}	The labile dissolved organic matter decay rate, s^{-1}
K_{LPOM}	The labile particulate organic matter decay rate, s^{-1}
K_{RDOM}	The refractory dissolved organic matter decay rate, s^{-1}
K_{RPOM}	The refractory particulate organic matter decay rate, s^{-1}
K_{NH4}	The nitrification rate, s^{-1}
K_{NO3}	The denitrification rate, s^{-1}
K_{s}	The sediment decay rate, s^{-1}
Sed_{NH4}	The sediment ammonia release rate, $m^{-2}gm^{-3}s^{-1}$
S_{od}	The anaerobic sediment release rate, $m^{-2}gm^{-3}s^{-1}$
P_{i}	Half saturation coefficient for phosphorus or nitrate and ammonia-nitrogen, gm^{-3}
P_{p}	The adsorption coefficient, $m^{3}g^{-1}$
δ_{N}	The stoichiometric coefficient for nitrogen
δ_{p}	The stoichiometric coefficient for phosphorus
Δ_{z}	The model cell thickness, m
γ_{om}	The temperature rate multiplier for organic decay
λ_{i}	Alga-growth limiting factor due to nutrients, i = phosphorus or nitrogen
λ_{l}	Alga-growth limiting factor due to light
ω_{a}	The alga settling rate, ms^{-1}
Φ_{a}	The alga concentration, gm^{-3}
Φ_{i}	Phosphorus or nitrate and ammonia-nitrogen concentration, gm^{-3}
Φ_{LDOM}	The labile dissolved organic matter concentration, gm^{-3}
Φ_{LPOM}	The labile particulate organic matter concentration, gm^{-3}
Φ_{RDOM}	The refractory dissolved organic matter concentration, gm^{-3}
Φ_{RPOM}	The refractory particulate organic matter concentration, gm^{-3}
Φ_{NH4}	The ammonium concentration, gm^{-3}
Φ_{NO3}	The nitrate concentration, gm^{-3}
Φ_{p}	The phosphorus concentration, gm^{-3}
Φ_{s}	The sediment concentration, gm^{-3}
λ_{min}	The multiplier for limiting growth factor where (minimum value of light, and nutrient) necessary for the growth are incorporated
γ_{ar}	Temperature rate multiplier for falling limb of curve
γ_{af}	Temperature rate multiplier for raising limb of curve
γ_{NH4}	Temperature rate multiplier for nitrification
γ_{NO3}	Temperature rate multiplier for denitrification

2.2 Model input data and initial and boundary conditions

The initial values of the constituents' concentrations and temperature were estimated at all grid points in the calculation domain by interpolation and extrapolation of observed values at points A13, A5, A7, A10 and A14 shown in Fig. 3. The simulation was started on April 1 in 1998. The utilized observed values were those acquired routinely, either once or twice a month, by local and national government[6].

To specify various values at the boundaries of the down-stream, up-stream, and water surface, observational data on water quality, water surface elevation, and meteorology were utilized.

The downstream elevation was given hourly by the average of water surface elevations at three places near Mikawa Bay (data by Japan Oceanography Agency[7]), i.e., Maisaka, Toba, and Nagoya (for example, see Fig. 7b). Temperature, salinity, and constituents' concentrations at point A14 observed monthly[6] were utilized to specify those values at downstream (ocean) boundary. Temperature and constituent concentrations were assumed to vary linearly in time between monitoring events. Vertical profiles of these state variables at the boundary were generated through interpolation and extrapolation of the observed data[6] at near-surface (i.e., 0.5 m below the surface) and middle (5 m below the surface) layers.

The two rivers and two waste water treatment plants (WTPs) were treated as tributaries. Time varying input data from rivers and waste water plants such as water qualities, water temperature, and fresh water loading were used for the upstream boundary. Daily fresh water loading from Toyokawa River was provided by the Toyohashi Office of Ministry of Land, Infrastructure and Transport, Japan[8], while water qualities such as TN, TP, and chlorophyll-a, and water temperature collected by local and national governments[6] were available on monthly basis. The data of Umedagawa River were also given monthly[6]. On discharge from WTPs, the flow rate, temperature, and nutrient concentrations were provided by the city of Toyohashi[9]. All these data were processed to daily values by temporal interpolation. Inputs from Toyokawa River and Noda WTP were introduced at 2 to 3 layers of segment 2, while those from Umedagawa River and Nakashima WTP were at 2 to 3 layers of segment 6. (See subsection 2.2 and Fig. 4 for the "segment" and "layer").

Hourly meteorology data such as wind velocity, air temperature, dew point temperature, and cloud cover index by Japan Meteorological Agency[10] were used as inputs to the model. Solar radiation flux is automatically calculated by using cloud cover index together with information on the location and time. Average of the meteorological data at both Toyohashi and Irago (Atsumi Peninsula) stations were used for the entire study area since both sites are located near the mouth of Toyokawa River and the outlet of Mikawa Bay (Atsumi Bay), respectively.

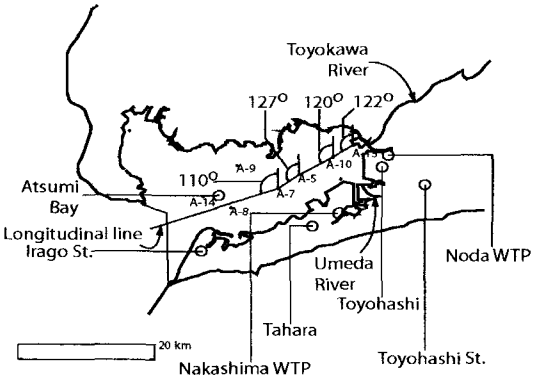

Fig. 3. The segmentation model of Mikawa Bay; the thick solid line indicates longitudinal axis in two-dimensional model; A5-A14 show monitoring points. Two waste water treatment plants are shown as "Noda" and "Nakashima" WTPs. Two AMeDAS (Automatic Meteorological Data Acquisition System) stations are also indicated as "Toyohashi St." and "Irago St."

2.3 Grid segmentation and simulation period

In this study, the water body of Atsumi Bay (i.e., the eastern half of Mikawa Bay) was simplified in a 2-dimensional space with longitudinal and vertical axes. As shown in Fig. 3, the longitudinal direction was set along the line connecting monitoring points A13, A10, A5, A7 and A14. As explained in subsection 2.1, all the 3-dimensional partial differential equations in the model were integrated laterally so that they were reduced to their 2-dimensional forms in space.

The water body along the longitudinal line was discretized into 30 equally spaced longitudinal segments and 24 vertical cells at the deepest place as shown in Fig. 4. Each segment had the same length of 855 m and each cell had uniform thickness of about 1.1 m. As shown in Fig. 4, each middle segment had multiple active cells and two boundary cells, i.e., one at the sea surface and another at the bottom of the sea; the thickness of the surface boundary cell was varied so that a rising or falling water surface could be accommodated, while the bottom boundary cell did not have thickness. The depth of segment below the surface boundary cell varied from 6.6 m (6 active cells) to 24.2 m (22 active cells). The inshore segment was divided into 8 cells with 6 active cells and the outer segment was divided into 24 cells with 22 active cells. The inshore segment near the mouth of Toyokawa River corresponded to the measurement point A13 (Fig. 3) and the point A14 was located at the outer segment near the open sea. Table 2 lists the correspondence of each measurement point to segment number in the grid calculation.

The numerical simulation was done for three years from 1 April, 1998 to 31 March, 2001, with time step for integration of 350 s. In this study, the results for about two months from May to early July in 1998 are focused.

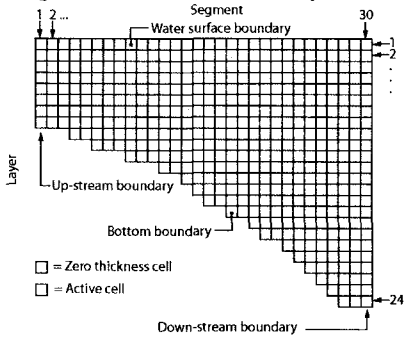

Fig. 4. Grid system for numerical calculation of Mikawa Bay. Length of "segment" is 850 m, and depth of "layer" is 1.1 m.

Table 2. Correspondence of locations: measurement points to grid segments.

Measurement point	Grid location
A13	Segment 2
A10	Segment 5
A5	Segment 11
A7	Segment 16
A14	Segment 29

3. RESULT AND DISCUSSION

To clarify the factors regulating the growth of alga, we focused on specific periods of high and low primary production; the days of 20 June and 4 July were chosen for the examples of the low and high productions, respectively. Temporal changes of TN, chlorophyll-a, bay water temperature, input river flow rate, and tidal height during two months (May, June, and early July) prior to algal bloom were analyzed.

3.1 Long term comparison of model simulation with observation

To see briefly the performance of the model calculation, observation and simulation were compared on chlorophyll-a. Figure 5 shows the temporal variation of observed (open circle) and calculated (solid line) chlorophyll-a in near surface water at segment (a) 2, (b) 11, and (c) 29; these segments correspond to measurement points A13, A5, and A14, respectively (see Fig. 3 and Table 2). The observation of chlorophyll-a in near surface layer was made at about 1 m below mean sea-surface level. In general, the model calculation reproduced reasonably well the seasonal variation found in the observation, although on several occasions the model failed in prediction of peak chlorophyll-a concentration (algal bloom).

3.2 Temporal variations of TN, chlorophyll-a, river flow rate, and temperature in early summer from May to July, 1998

Based on the quantitatively reasonable simulation results in 3.1, we will use the calculated results to clarify the factors controlling algal bloom in Mikawa Bay (actually, Atsumi Bay). For this purpose, we focus on a period from 20 June to 6 July in 1998 in which high chlorophyll-a concentration was observed on 6 July and also high river flow rate occurred on 20-24 June prior to bloom. To see seasonal trend during the target period, the temporal variations of the calculated TN, chlorophyll-a, and ammonium are plotted from 1 May to 6 July with 6 hours interval in Fig. 6. Similarly, Fig. 7a presents those of the observed river flow rate (Toyokawa

River), and the simulation-derived sea water flux from and to the inner bay, while Fig. 7c is the calculated temperature at layer 6 (about 5.5 m below the surface) of segment 2. Figure 7b illustrates the temporal variation of the input tidal height from 00LST on 20 June to 00LST on 6 July at the downstream boundary.

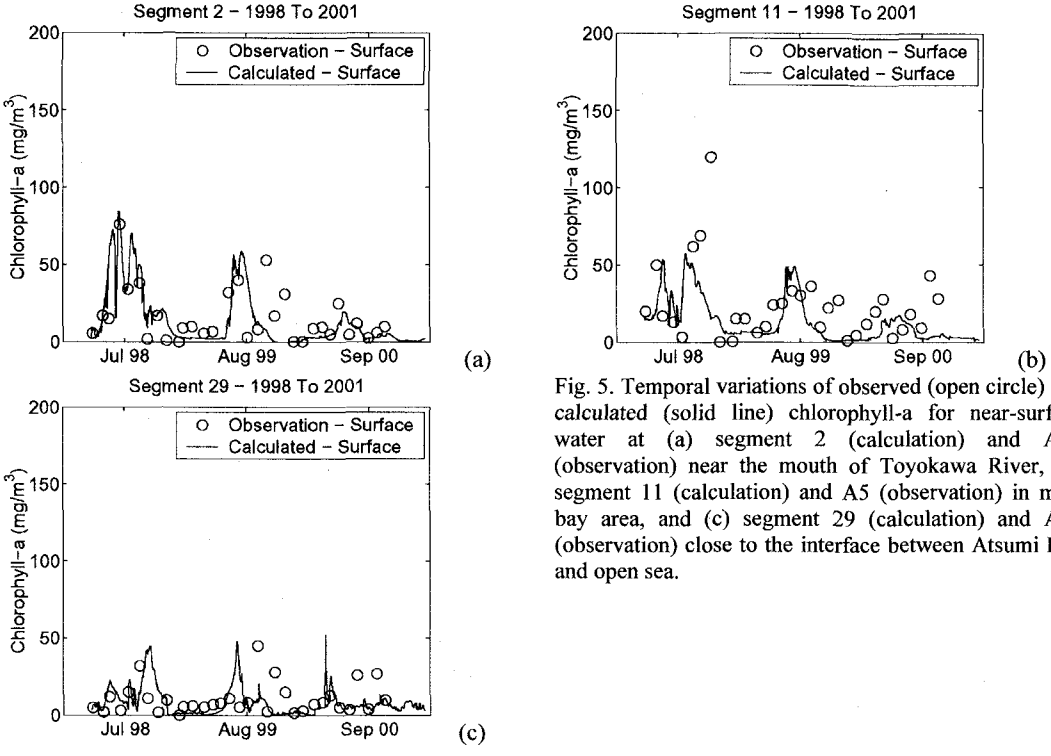

Fig. 5. Temporal variations of observed (open circle) and calculated (solid line) chlorophyll-a for near-surface water at (a) segment 2 (calculation) and A13 (observation) near the mouth of Toyokawa River, (b) segment 11 (calculation) and A5 (observation) in mid-bay area, and (c) segment 29 (calculation) and A14 (observation) close to the interface between Atsumi Bay and open sea.

As suggested in Fig. 7b, both days of 20 June and 4 July were the neap tide day, and the exchange of sea water between the inner and outer bay areas was relatively small on these day, (see the solid and open bar in Fig. 7a).

Figures 6a,c indicate TN near the surface layer shows large variation in short time span and has slightly-increasing trend on a monthly basis, while TN near the bottom layer in Fig. 6b, d indicates rather monotonic increase with time. The large TN variation at the surface is attributed to the increased TN loading due to increased river flow rate shown in Fig. 7a; for example, the increase of TN concentration in the surface water from 20 June to 26 June at segment 2 (Fig. 6a) and 6 (Fig. 6c) is synchronized with the large river flow rate during the same period in Fig. 7a. The TN variation is relatively small and smooth at segment 6, which is in distant area of about 5 km from the river mouth. In contrast to this surface TN, the TN concentration at the bottom layer (Fig. 6b, d) shows rather monotonic increase. Since variation of the ammonium concentration in Fig. 6b, d is similar to that of the TN in the bottom layer and furthermore nitrogen is released primarily as ammonia from the sediment and then oxidized to nitrate (see Fig. 2), the trend of TN can be regarded as formed mainly due to enhanced decay of sediment and enhanced ammonia release from the sediment with increased temperature (Fig. 7c). This steady increase may also suggest rather poor flushing rate of sea water in the inner bay area; we will discuss this point later.

Chlorophyll-a at surface level is also largely affected by river flow rate, although in contrast to TN, chlorophyll-a at surface decreases when river flow rate is large; relatively low chlorophyll-a concentration in the river water contributes to this. Figures 6a, c also show that chlorophyll-a concentration generally increases from 1 May to 6 July. The increase reflects enhanced solar radiation and raised sea water temperature together with the increased TN concentration. Then, the fluctuation of chlorophyll-a concentration due to large river flow rate is superimposed on this monthly increasing trend. As does the TN bottom concentration, chlorophyll-a in the bottom also monotonically increases at segment 2 (Fig. 6b) and 6 (Fig. 6d).

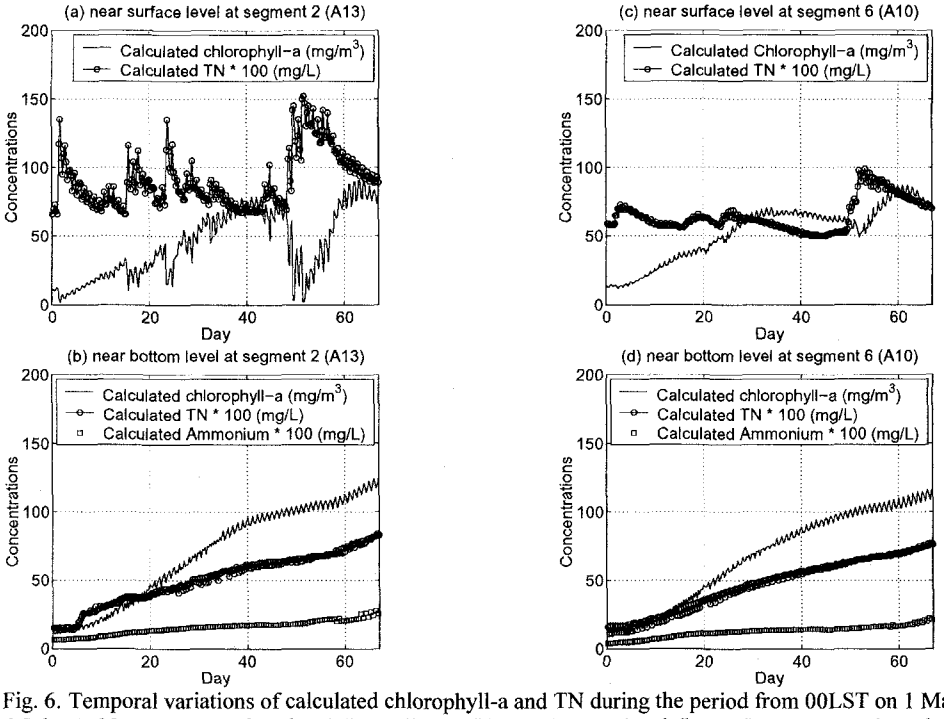

Fig. 6. Temporal variations of calculated chlorophyll-a and TN during the period from 00LST on 1 May to 00LST on 6 July, 1998: (a) near-surface level (layer 2) and (b) near-bottom level (layer 6) at segment 2, and (c) near-surface level and (d) near-bottom level (layer 7) at segment 6.

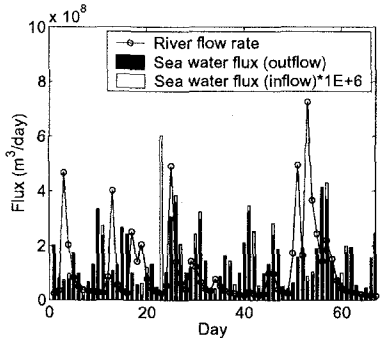

(a)

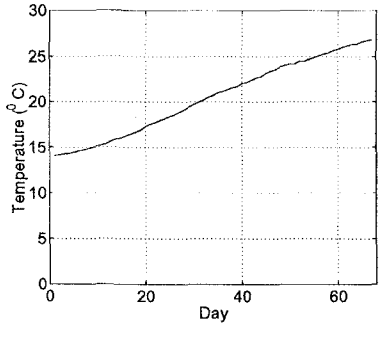

(c)

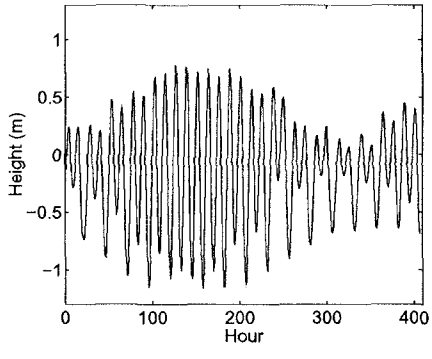

(b)

Fig. 7. Temporal variations of (a) river flow rate and sea water fluxes at segment 6. (i.e. the fluxes into and out-of the inner bay area) are expressed with open- and solid-bars, respectively, (b) tidal height, and (c) temperature near the bottom (layer 6) at segment 2. In Figs. 7 (a) and (c) the "day" starts from 1 May and continue to 6 July, 1998, while in Fig. 7 (b) the "hour" begins at 00LST on 20 June and ends at 00LST on 6 July, 1998.

3.3 Characteristics of chlorophyll-a, TN, TP, flow, temperature, and salinity on the days of high and low river flow rates

With the background on the long term trends of the variables during 1 May to 6 July 1998, we further selected two days of 20 June and 4 July, 1998 for a detailed analysis, since observed data in Fig. 5 showed that chlorophyll-a concentration was very high on around 4 July, 1998 (Julian day 186) and moderate on 20 June, 1998 (Julian day 172). We also thought that the time difference of about two weeks (i.e., about a half of a typical lunar month) between 20 June and 4 July was not too bad to compare, since climatic change such as air temperature might not be so large and the tidal condition shown in Fig. 7b was quite similar; a daily averaged height of the sea surface at segment 29 was -0.18 m on both days. These two days had also distinct characteristic on their input fresh water flow rates; that is, the daily averaged flow rate was very high at 495 m^3/s on 20 June and low at 19 m^3/s on 4 July. In Fig. 8, vertical cross sections of daily averaged variables are illustrated: (a) velocity, (b) chlorophyll-a, (c) TN, (d) TP, (e) temperature, and (f) salinity; in the figure the left panels are for 20 June, and the right panels for 4 July. Since both 20 June and 4 July were rather the neap tide days (as can be inferred from Fig. 7b), the daily averaged flows of Figs. 8a and b do not show significant residual flows and thus notable exchange of sea water mass between the inner bay (segment number <10) and the outer bay can not be expected. However, in contrast to 4 July, there was large inflow of river water on 20 June (Fig. 8a), and this induced relatively strong surface flow together with its secondary flow in the inner bay (Fig. 8a). Hence the exchange of sea water can be thought larger on 20 June, though it might not be so significant. Suzuki and Terasawa[1)] and others pointed out formation of the estuary circulation induced by increased river flow rate, though the formation seems to be not so remarkable in Atsumi Bay in their summer condition[1)].

We also additionally tested the effect of river flow rate on the circulation. Since it may be noted that the applied model is laterally integrated 2 dimensional one, there may be limitation on its ability. First, we performed a simulation with the same conditions as the normal case but without tide. Then a clear circulation extending from segment 2 to 10 on vertical plain (see Fig. 8a for the segment's location) was formed on 20 June, i.e. the day of large river flow rate, but not on 4 July with low river flow rate. Next, we did the same simulation with tide but specifying lower temperature at the surface water compared with that at the bottom. This implies the stable stratification was weakened (the salinity condition was kept to be the same), and thus more vertical exchange of momentum possibly occurred. In this case, the relatively strong circulation was also formed on 20 June and weak one even on 4 July. Judging from these results, we suppose that the formation of the circulation associated with input of river flow tends to occur under not strong but weak stable stratification and is closely affected by tidal condition. (We did not calculate Richardson number explicitly, and thus quantitative evaluation on the condition for the formation of the circulation is left uncertain). As for the days of 20 June and 4 July (Fig. 8a) and the period between these days, both temperature (Fig. 8e) and salinity (Fig. 8f) showed strong stable stratification in the bay. Hence the intensive circulation on 20 June (the left panel of Fig. 8a) was not seen.

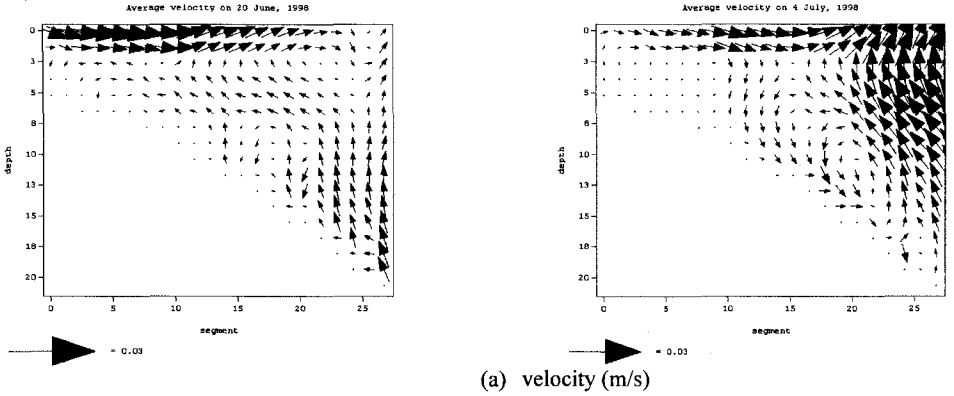

(a) velocity (m/s)

Fig. 8. Vertical cross sections of the calculated (a) velocity field, (b) chlorophyll-a, (c) TN, (d) TP, (e) temperature, and (f) salinity on 20 June (left panel) and 4 July (right panel) in 1998. The length of one horizontal segment is 855 m, and the depth of one vertical cell is 1.1 m.

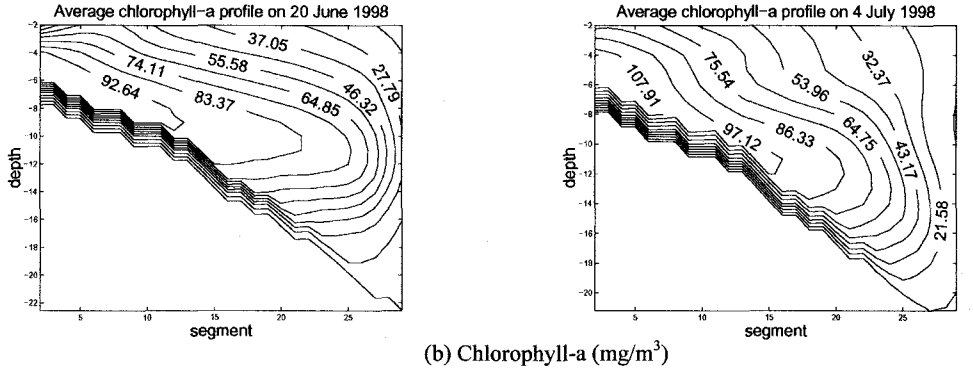

(b) Chlorophyll-a (mg/m^3)

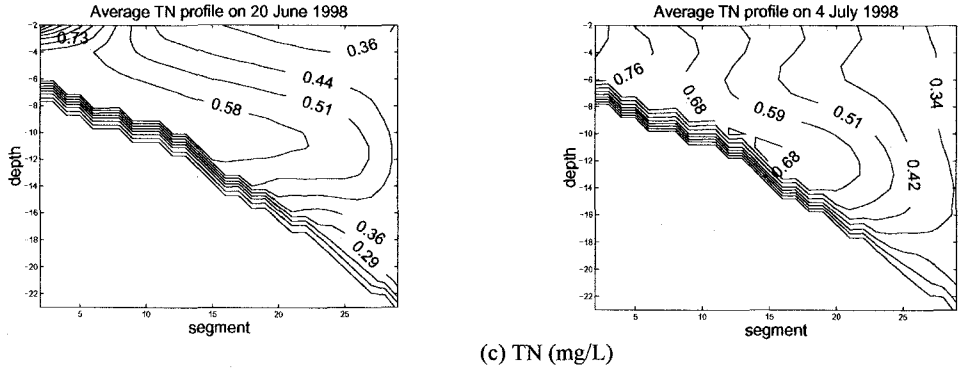

(c) TN (mg/L)

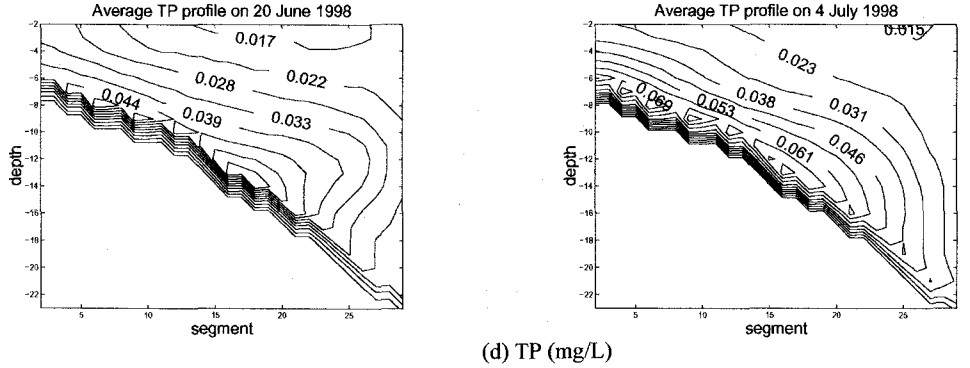

(d) TP (mg/L)

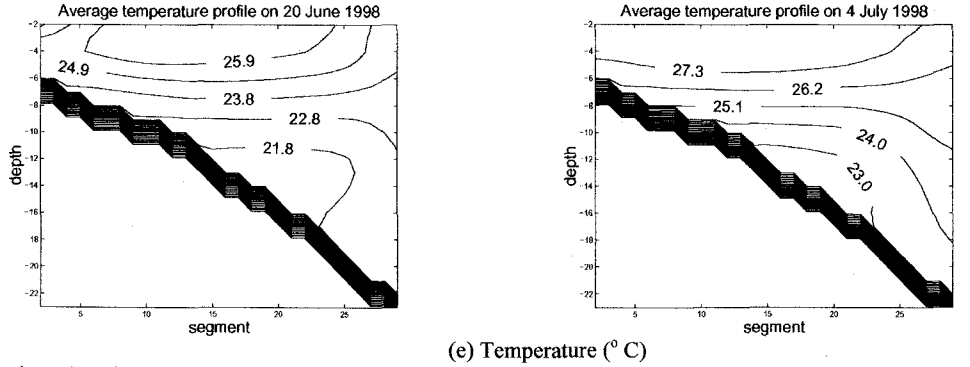

(e) Temperature (^{o} C)

Fig. 8 (continued)

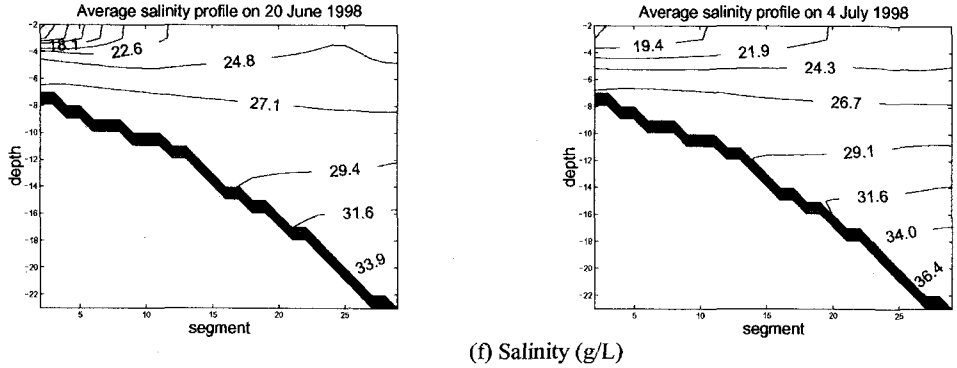

(f) Salinity (g/L)

Fig. 8 (continued)

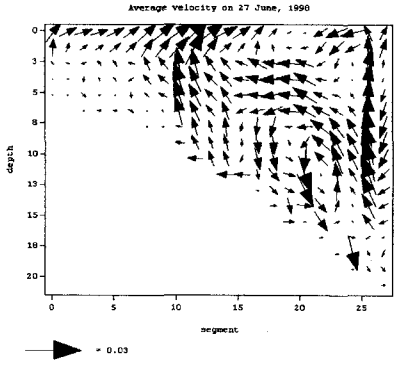

Fig. 9. Daily averaged velocity field during the flood tide on 27 June, 1998.

It may be noted that under the stable condition found during 20 June to 4 July, even on a flood tide day, the mass exchange of sea water between the inner bay and outer bay may not be large in Atsumi Bay; for example, the daily averaged flow (see Fig. 9) on the flood tide day of 27 June (see the tidal height in Fig. 7b) suggests strong net tidal effect on the mass exchange can be expected only in the outer bay area (segment number>10).

This is probably due to the topography of the bay floor; the slope of the bay floor is quite steep in the outer area (segment 12-29), and changes sharply to a gentle one in the shallow bay area (segment 2-10); thus, for strong up-tide condition, a convergence, and thus upwelling is formed over the segment 10-14 and the exchange of bay water between the outer and inner areas is suppressed. The upwelling in the middle of bay over segment 10-14 in Fig. 9 is also pointed out by other researches (Suzuki and Matsukawa[11]; Suzuki[12]). As can be seen in Fig. 8e, during the two weeks from 20 June to 4 July, the bay water temperature had been raised by more than 1.4 °C at the surface layer and by 1.2 °C at the bottom where the lowest temperature in the bay occurred. Thus the temperature difference between the surface and bottom layers had been enhanced toward even more stable stratification. In the temperature profile on 20 June (the left panel in Fig. 8e), vertically uniform temperature at the small area near the river mouth can be found. This may be due to the high flow rate from the land area (495 m^3/s). Moreover, as can be seen in Fig. 8f, the salinity difference between the surface and middle/deep layers had been enhanced toward stable condition for the two weeks from 20 June to 4 July. As seen above, both temperature and salinity had changed their vertical profiles so that the stable condition was enhanced during the two weeks. This stable stratification also contributed to the high chlorophyll-a on 4 July by further suppressing vertical mixing of the sea water.

4. CONCLUSION

In this study, we have numerically investigated eutrophication and algal bloom in Atsumi Bay (i.e., the eastern half of Mikawa Bay) by focusing on specific period in early summer, 1998 and clarified the factors regulating the chlorophyll-a production. The obtained results are as follow:

(1) Two month analysis showed concentrations of TN and chlorophyll-a near the bottom layer in the shallow area had continuously increased from the beginning of May to early July (Fig. 6b, d). Enhanced TN release from the sediment by increased temperature and enhanced photosynthesis by solar activity were thought to be the reasons.

(2) TN and chlorophyll-a near the surface layer had strongly been affected by river flow rate; the TN concentration showed its sharp increase when the river flow rate increased, and in contrast to TN, the chlorophyll-a decreased for the increased river flow rate; these are because of high TN and low chlorophyll-a concentrations in the river water. After the end of the high river flow rate, the TN gradually decreased and on the other hand, chlorophyll-a increased (Fig. 6a, c). During the two months, the TN concentration at the surface layer had not shown clear trend of its increase (Fig. 6a, c), while in contrast, the chlorophyll-a had increased on average.

(3) Tidal condition affected exchange of sea water between inner and outer bay areas with the large exchanged mass at the flood tide and small at the neap tide (Fig. 7a, b).

(4) The reason of high chlorophyll-a concentration on around 4 July was concluded as follows: TN release from the sediment in the shallow area was enhanced day by day because of increased temperature; in addition, there was large influx of TN through rivers during 19 to 27 June; the accumulated TN had long residence time in the shallow area of the inner bay due to weak ventilation of the sea water under the neap tide condition from around 29 June to 5 July, and thus biological reactions could have enough time to trigger algal bloom.

(5) The reason why the large river flow rate on 20 June did not induce visible circulation in the inner bay area may be attributed to strong stable stratification caused by high temperature in the surface water during the period.

REFERENCES

1) Suzuki, T., and Terasawa, T. (1997) A simulated, numerical reproduction of an oxygen-depleted water mass in a eutrophic estuary; and an examination of methods to increase the oxygen concentration in depleted waters: The case of Ise and Mikawa bays. *J. Adv. Mar. Sci. Tech. Soci.*, **3**, 81-102.
2) Sohma, A., Sekiguchi, Y., Yamada, H., Sato, T., and Nakata, K. (2001) A new coastal marine ecosystem model study coupled with hydrodynamics and tidal flat ecosystem effect. *Marine Pollution Bulletin*, **43**, 187-208.
3) Cole, T.M., and Wells, S.A. (2000) *User Manual- CE-QUAL-W2: A Two Dimensional, Laterally Averaged Hydrodynamic and Water Quality Model*, Version 3.0, U.S. Army Corps of Engineers Washington, DC; http://www.coe.uncc.edu/~jdbowen/neem/w2_v2_manual.pdf.
4) Anggara Kasih, G.A., and Kitada, T. (2003) Analysis of water quality response to nutrient loading and sediment resuspension at Mikawa Bay. *Preprint Volume of Annual Meeting of the Chubu Branch*, Japan Society of Civil Engineers, Toyohashi, March 7, 2003, 657-658.
5) Anggara Kasih, G.A., and Kitada, T. (2004) Numerical simulation of water quality response to nutrient loading and sediment resuspension in Mikawa Bay, central Japan: Quantitative evaluation of the effects of nutrient reduction measures on alga blooming. *Hydrological Processes*, **18** (in press).
6) Division of Environment, Aichi Prefecture Office, Japan (1999) *Report on the Water Quality at Public Water Area for 1998 (Kokyo-yo Suiiki-tou Suishitsu-chosa Kekka)*, 270p. (in Japanese).
7) Japan Oceanography Data Center (2002) http://www.jodc.go.jp/onlinedata/tide.
8) Toyohashi Office, Ministry of Land, Infrastructure and Transport, Japan (2002) *Data on river flow rate of Toyokawa River for 1998-2001* (in Japanese).
9) Toyohashi City Office (2002) *Data on sewage water treatment system in Higashi Mikawa for 1998-2001* (in Japanese).
10) Japan Meteorological Agency (2002) *AMeDAS (Automatic Meteorological Data Acquisition System) Data for 1998-2001*, CD-ROM.
11) Suzuki, T., and Matsukawa, Y. (1987) Hydrography and budget of dissolved total nitrogen and dissolved oxygen in the stratified season in Mikawa Bay, Japan. *Journal of the Oceanographical Society of Japan*, **43**, 37-48.
12) Suzuki, T. (2001) Oxygen-deficient waters along the Japanese coast and their effects upon the estuarine ecosystem. *J. Environmental Quality*, **30**, 291-302.